

Radiation Emission Correlated with the Evolution of Current Sheath from a Deuterium Plasma Focus

M. Shahid Rafique · P. Lee · A. Patran ·
R. S. Rawat · S. Lee

© Springer Science+Business Media, LLC 2010

Abstract The time resolved emission of neutrons and X-rays (both soft and hard) is correlated with the current sheath evolution during the radial phase of a 3.2 kJ Mather-type plasma focus device operated in deuterium at an optimised pressure of 4 mbar. A three-frame computer-controlled laser shadowgraphy system was incorporated in the experiment to investigate the time evolution of the radial phase of the plasma focus. The dynamics of the sheath was then correlated with the time resolved X-rays and neutron emission. The time-resolved neutron and hard X-ray emission was detected by a Scintillator-photo-multiplier system while the time resolved soft X-rays were detected employing filtered PIN photo diodes. The observations were recorded with a temporal accuracy of a few ns. For the reference, the total neutron yield was also monitored by an Indium Foil activation detector. The correlation with the High Voltage Probe signal of the discharge, together with the X-ray and neutron emission regimes enabled to identify the important periods of the sheath evolution i.e. the radial compression (pre focus), minimum pinch radius (focus) and the post focus phenomena. During the initial stage of the radial phase, velocities of 10–23 cm/ μ s, while at the later stage of the radial phase (up till the compression), velocities up to 32–42 cm/ μ s were measured in our experiment. For the

discharges with the lower neutron yield (lower than the average value $\sim 1 \times 10^8$ n/discharge), the current sheath appears to be disturbed and neutron and hard X-ray signal profiles do not carry much information whereas the soft X-ray emission is significant. For the discharges with high neutron yield (higher than the average value), the current sheath has a smooth structure until the maximum compression occurs. Hard X-ray emission is maximum for the discharges with high neutron yield, especially whenever there is development of $m = 0$ instability compressing the column to very high densities. The neutrons are emitted long after the maximum compression supporting the beam target fusion. For the discharges with High neutron yield, the soft X-ray production is less as compared to the discharges with low neutron yield.

Keywords Plasma focus device · Hard X-rays · Soft X-rays · Neutrons

Introduction

Plasma Focus (PF) device is capable of producing a short lived, high density plasma. The pinched plasma leads to the emission of radiations such as neutrons (operated in deuterium) [1] X-rays (both soft and hard) [2–6] and ions [7]. In the DPF device a current sheath is formed in the vicinity of insulator sleeve (breakdown phase). An azimuthal magnetic field is established as a result leading towards the formation of a Lorentz force. Due to this force the sheath moves in the axial direction along the anode (axial acceleration phase). The next sequential phase is the radial phase in which the current sheath moves in a radial direction towards the centre of the anode tip until it reaches the centre and collapses (the pinch). The imaging of the

M. S. Rafique · P. Lee · A. Patran · R. S. Rawat · S. Lee
Natural Science and Science Education Academic Group,
National Institute of Education, Nanyang Technological
University, 1-Nanyang Walk, Singapore 637616, Singapore

Present Address:

M. S. Rafique (✉)
Department of Physics, University of Engineering
and Technology, Lahore 54890, Pakistan
e-mail: shahidrafique@uet.edu.pk

plasma sheath structure and its dynamics during the radial phase is of vital interest in knowing the actual behaviour and variety of phenomena taking place in the plasma. Different studies were made in the past to investigate the current sheath dynamics and related phenomena. The structure of the pinched column for small plasma focus devices (≤ 10 kJ) was investigated by several authors [8–12]. It was found that in small scale experiments, the primary filamentation of the current sheath is destroyed during the collapse phase, when a plasma column of a few millimetres in diameter is formed [9]. Yamamoto et al. [13] studied the neutron production mechanism through the time correlation between the dynamic behaviour of the focused plasma and the burst of the deuteron beams, X-rays and neutrons. Toshikazu et al. [14] suggested that the generation of the ion and the electrons beam occur in an interval of 20 ns around the peak of the voltage spike and the plasma inductance increases monotonically, but rather slowly during the process of the $m = 0$ instability growth. Comisar [15] suggested that the lifetime of the resulting fountain like pinch column appear to be governed by the formation of sausage instabilities. Nevertheless, the build up time of the $m = 0$ instabilities are at least 5–10 times shorter than the observed pinch lifetime (~ 50 ns).

The structure and the time dependent evolution of the sheath is responsible to set the emission parameters of the radiations like neutrons and X-rays.

Mohammadi et al [16] correlated the time resolved soft X-ray emission with the dynamics of the sheath by increasing the length of the conventional anode.

In this paper, the current sheath structure, dynamics and its influence on the radiation emission during the radial phase of a 3.2 kJ Mather-type plasma focus is presented. The dynamics during the radial phase of the sheath is correlated with the time resolved emission of radiation (neutron and X-rays) along with high voltage probe signal profiles.

Experimental Set-up

The experiments were carried out on a 3.2 kJ Mather type plasma Focus device. The device was operated with a 33 μ F/14 kV capacitor giving a discharge current of about 180 kA (a typical Rogowski Coil signal). The main tube of the device consists of a cylindrical copper anode of 1.9 cm in diameter with 16 cm length surrounded by 6 equally spaced copper cathode rods making a diameter of 6.4 cm concentric with the anode. The insulation between the cathode and anode is provided by a glass insulator sleeve.

The device was operated in deuterium at an optimised pressure of 4 mbar.

In order to investigate the radial phase of the plasma focus evolution three shadowgraphic images of a single discharge of the device were captured. A CCD based three-frame computer-controlled laser shadowgraphy system was employed in the experiment. The first part of the shadowgraphy system was a three locally fabricated nitrogen dye lasers (used as probe beams) synchronized with a few nano second accuracy with an appropriate delay (a few ns) between each pulse to capture three images of a single shot of plasma focus device [17]. The second part was a telescopic arrangement for image resolution to fit to the field of view of the CCD. The third part was the video capture system comprising of a data acquisition and transfer facility. The triggering of the CCD was done internally by transferring the image to the disk when there was a significant increase in the light level. The timing between the probe laser and the discharge was adjusted using the laser pulse and the high voltage signal. A schematic of the shadowgraphy system is shown in Fig. 1a. A detailed description of the system can be found in [17].

The images obtained thus were then correlated with the time resolved neutron, hard X-ray and soft X-ray emission. A scintillator-photomultiplier system was used to explore the time resolved behaviour of neutrons and hard X-rays. The detector consisted of a plastic scintillator (NE 102A of 50 mm diameter and 40 mm thickness) and a photomultiplier (EMI 9813B) tube. The plastic scintillator was wrapped in an Aluminum foil, with the exception of the side facing towards the window of the photomultiplier tube. For proper optical coupling, Dow Corning 200 silicon grease was used between the plastic scintillator and the tube.

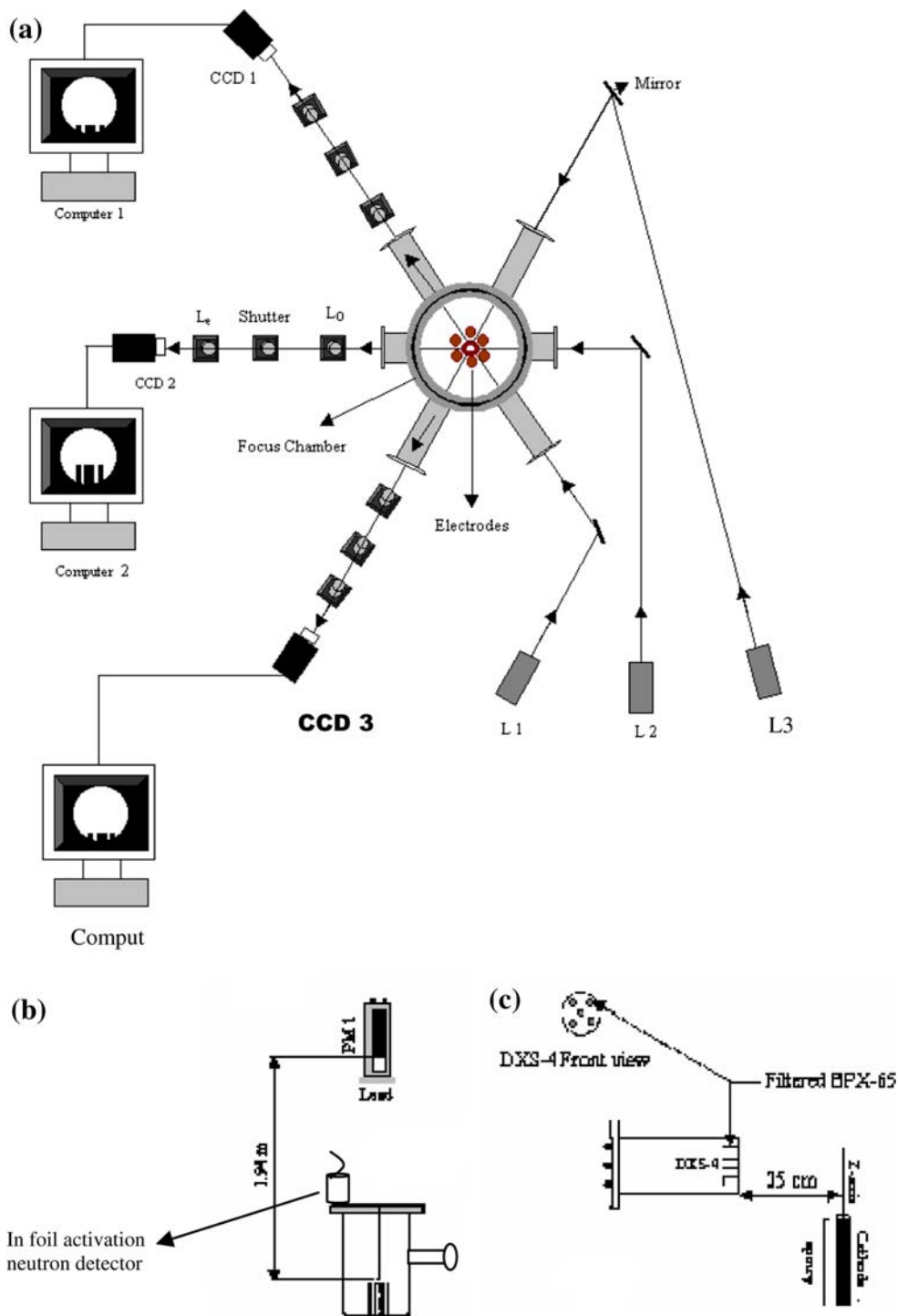
The detector, referred to as PM1, was placed at a distance of 1.94 m in the axial direction at 0° with respect to the pinch (Fig. 1b). To cut off most of the hard X-rays or to avoid the saturation of the tube, lead sheets (3 mm thick) were placed in front of PM1. The neutron time of flight from the pinch to the PMT was also compensated to synchronize with the Hard X-ray timings. The total neutron yield was measured with the help of an Indium foil activation detector (BICON). The calibration factor for the detector was found to be 1.5×10^5 neutrons/count [17].

For the time resolved soft X-ray measurements two of a five-channel soft X-ray spectrometer (*DXS-4*) was used the details of which can be found in [17, 18]. The arrangement is shown in Fig. 1c. The data was acquired on a ten channel HP 250 MHz Oscilloscope.

Results and Discussion

In order to investigate various phenomena involved in the focus dynamics when operated in deuterium at an optimised

Fig. 1 **a** A set up for the three frame shadowgraphy system (*top view*). **b** A schematic of a Scintillator-photomultiplier system for the time-resolved neutron and hard X-rays measurements along with the In foil activation detector for total neutron yield measurements. **c** A schematic of the arrangement for time resolved soft X-ray measurements



pressure of 4 mbar and to identify their role in the radiation emission, the radial phase is classified as: (1) Pre-focus Phase, (2) Focus Phase and (3) Post Focus phase. This classification is based on the time correlation between the high voltage probe signal and the probing laser beam signals. Time is taken $t = 0$ at the time of maximum compression indicated by the high voltage

pulse and is observed by the shadowgraphs. Time is assigned a negative value before focusing (maximum compression) and is positive after the maximum compression. For each phase the results are discussed with reference to the total neutron yield. The average neutron yield (taken for 5000 discharges) is found to be 1×10^8 n/discharge.

Pre-Focus Phase

This is the phase in which the current sheath starts from the open end (tip) of the anode and accelerates towards the centre. This phase ends when the current sheath meets the axis at the centre of the anode ($t = 0$).

Figure 2 presents a three-frame sequence of a single shot during pre-focus phase within a time span of -10 ns to -5 ns. The time resolved hard X-rays (HX), neutrons $(dY_N/dt)_{PM1}$, soft X-rays $(dY_{sx}/dt)_3$, $(dY_{sx}/dt)_4$ and high voltage probe (V) signal profiles of are also shown. The neutron yield for this shot is 4.5×10^7 lower than the average value. The voltage signal profile (V) shows multiple spikes indicating that the discharge belongs to the multiple-compression regime. This multiple compression might be due to the uneven transfer of energy from the capacitor bank. The experimentally measured radial velocity is $26 \text{ cm}/\mu\text{s}$ which is in agreement with the work done by Lee [19] and Zhang [20]. In the last frame ($t = -5$ ns), A slight breakage of the sheath appears (encircled) which might effect the focussing at the later stages. No significant information could be extracted from these images. The time resolved hard X-ray and neutron signal profiles do not show significant peaks. However, soft X-ray signal profiles $(dY_{sx}/dt)_3$ and $(dY_{sx}/dt)_4$ show that there is emission of soft X-rays but not at the first focus peak (V at $t = 0$). The emission starts 150 ns after the main focus and lasts for about 400 ns. This emission corresponds bremsstrahlung due to the presence of hot electron.

Figure 3 shows another discharge with total neutron yield of 3.6×10^7 (lower than the average value) during the pre-focus phase. It is again a multi-compression discharge as indicated by the High voltage probe signal (V). Almost after 150 ns, there is an onset of another

focussing event which lasts for about 150 ns. This multiple focus discharges are attributed to the weak setting up of the break down phase near the insulator sleeve surface. The current sheath seems to have a lower density and is much wider than the “normal” discharge. At the instant 1 ns before the maximum compression, the column is compressed at one point relatively far from the tip of the anode, while, near the tip of the anode the sheath is yet to reach the centre. The axial elongation of the plasma as well as the short radius of curvature of the sheath is observed. The low neutron yield could then be explained by a significant loss of the plasma in the axial direction (towards and away from the anode), which reduces the number of particles to be confined, thus, the final density and temperature might have low values. Experimentally measured average radial velocity for this discharge is $30 \text{ cm}/\mu\text{s}$.

The time resolved hard X-ray (HX) and neutron $(dY_N/dt)_{PM1}$ signals are flat. The reason could be attributed to the less dense sheath as it appears in the shadowgraph. The density at the maximum compression might not have reached the sufficient value to create hot electrons and strong ion beams. The soft X-ray production $(dY_{sx}/dt)_3$ and $(dY_{sx}/dt)_4$ are emitted with the first focussing of the sheath. 150 ns after the first focus there is another burst of the soft X-rays which corresponds to the second focussing event of the sheath. A very weak third emission is observed at 600 ns after the first focus which might be due to the sputtering of the copper anode.

A comparison of the two discharges with low neutron yield shows that the implosion speed alone is not a critical parameter for neutron production. The compression may be fast, but if the geometrical profile of the sheath favours significant losses, the confinement efficiency decreases.

Fig. 2 A three frame sequence of a discharge during the pre-focus phase along with signal profiles of dY_N/dt , dY_{HX}/dt , dY_{sx}/dt and V. The neutron yield for this shot is 4.5×10^7 lower than the average value

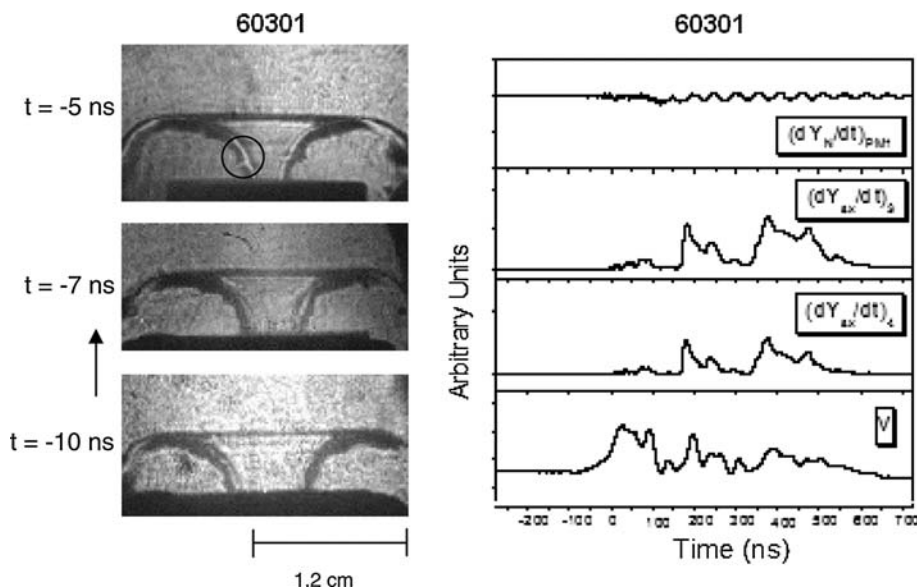


Fig. 3 A three frame sequence of a discharge during the pre-focus phase along with signal profiles of dY_N/dt , dY_{HX}/dt , dY_{sx}/dt and V . The neutron yield for this discharge is 3.6×10^7 (lower than the average value)

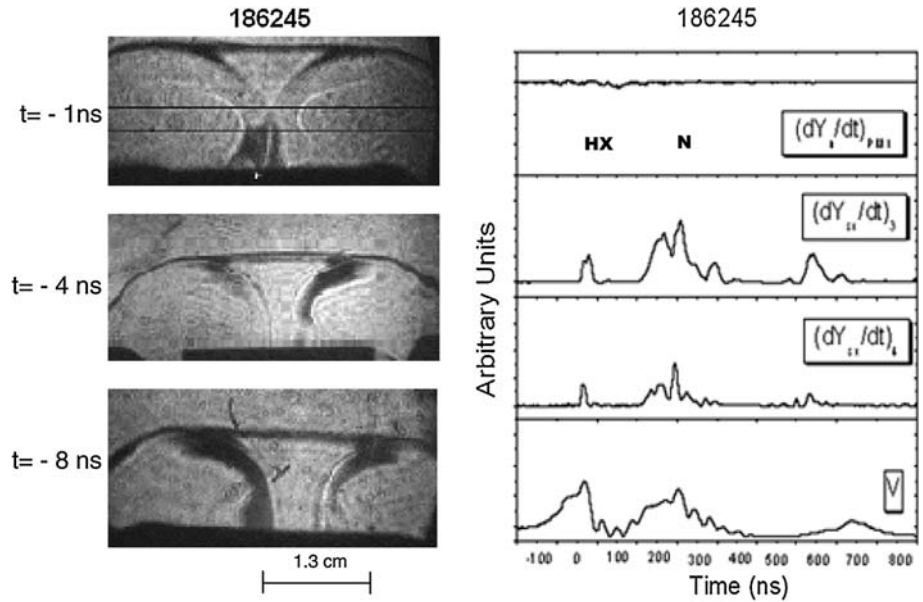


Fig. 4 A three frame sequence of a discharge during the pre-focus phase along with signal profiles of dY_N/dt , dY_{HX}/dt , dY_{sx}/dt and V . The neutron yield is 1.3×10^8 higher than the average value

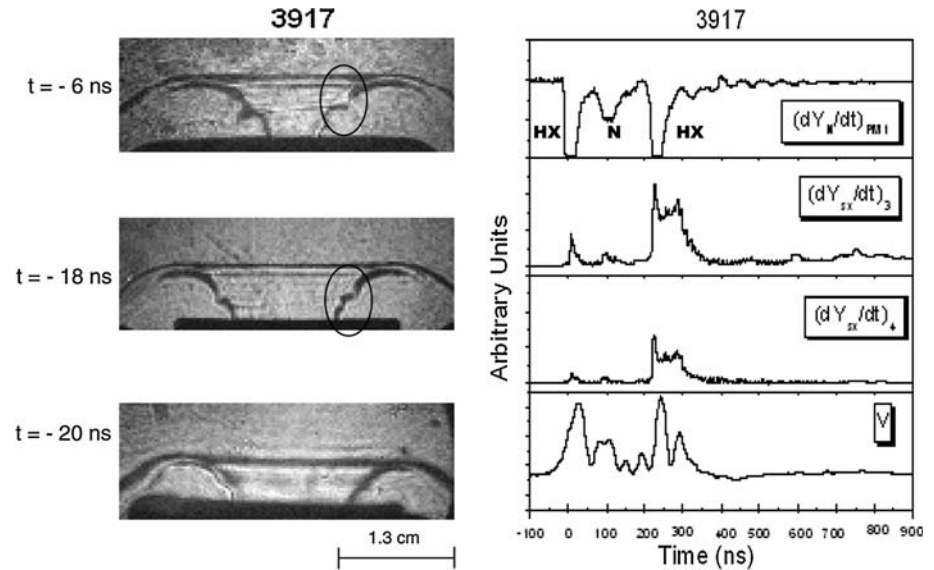


Figure 4 shows a three-frame sequence of a discharge exhibiting neutron yield 1.3×10^8 higher than the average value along with the time resolved signal profiles of hard X-rays (HX) and neutrons dY_N/dt , soft X-rays $(dY_{sx}/dt)_3$ and $(dY_{sx}/dt)_4$ and high voltage probe (V).

In this particular discharge, the development of RT instability (encircled) is seen on both the wings of the sheath. Normally, the growth of instability is associated with a high neutron yield and intense hard X-ray bursts. The average radial velocity for this discharge is 21 cm/ μ s.

The hard X-ray burst (HX) appears immediately at the first focus point ($t = 0$), the signal is saturated which means that intense burst of X-ray is emitted at this instant. Which might be attributed to the hot electrons which are generated immediately after the sheath is tightly focussed

and a very high dense compression is formed. There is emission of neutrons 100 ns after the maximum compression which corresponds to the first focussing event. The neutron signal lasts for about 70–80 ns. The reason for the delayed emission is due to the setting up of a self generated electric fields which causes the separation of the two major species of the plasma. Thus, an ion beam is formed emitted away from the anode tip. The ions undergo beam target fusion resulting in the emission of the neutrons.

Another burst of the hard X-rays observed 22 ns after the first peak which is due to the second focussing event as clearly seen from the voltage signal.

The soft X-rays are also emitted at the first focus point but the intensity is much lower especially of the signal from the 4th detector $(dY_{sx}/dt)_4$. The reason is quite

obvious that at the first focus, the whole of the electron contributed towards the emission of the hard X-rays but a little emission is in the soft X-ray range. However, at the second focus point about 200 ns after the first focus, the soft X-ray emission is quite significant. The reason could be related to the formation of the electron beam after the setting up of the self generated electric field in the plasma causing more collisions and generating more soft X-ray.

Focus Phase

The results presented in this section describe the shadow-graphs and signal profiles taken during and near the maximum compression of the current sheath.

Figure 5 shows a sequence of a three-frame shadow-graph, along with the corresponding time-resolved neutron, X-ray (soft and hard), current and voltage signal profiles. The discharge belongs to multiple-compression regime, as indicated by the voltage signal profile. Neutron yield for this discharge is 4.3×10^7 which is lower than the average value. The development of RT instabilities is seen on both the wings of the funnel shaped current sheath. The sheath seems to have less density. Hard X-ray (HX) and neutrons emission signals (N) are not identified which might be due to the less dense current sheath forming a wider plasma column at the focus point.

An intense burst of soft X-rays is observed. The strong soft X-ray emission is related to the emission of strong relativistic electron beams long after the maximum compression.

Figure 6 shows a sequence of a three-frame shadow-graph, and the corresponding time-resolved neutron, X-ray (soft and hard), current and voltage signal profiles with low

neutron yield (2.4×10^7) in which the development of $m = 0$ instability is clearly seen at the later stage (20 ns) after the pinch (top frame). At $t = 0$, there is the onset of the instability. It appears that the focussed column has not attained the optimum length after the maximum compression. That is why the shot does not have such a high neutron and hard X-ray emission even though there is appearance of the instability long after the maximum compression.

In Fig. 7, two unusual discharge are shown. The neutron yield is 7.4×10^7 quite near to the average. The sheath dynamics (Fig. 7a) seems to be normal during the initial stage (bottom frame), but, 1 ns before the compression the right wing of the sheath appears to move faster than the left one and the compression occurs in a very peculiar manner. It looks like that the column is formed somewhere inside the hollow anode. An RT instability disturbing the left wing can be seen in the middle and the top frames. In Fig. 7b (bottom and middle frames), the column seems to behave like a “tornado”. The column looks twisted and highly compressed at the tip of the anode (bottom frame). This kind of discharges is not commonly observed (only 5% of the recorded discharges). This might be due the onset of the $m = 1$ instability but the B field might not me so strong to let the $m = 1$ instability fully develop.

For the discharge with a very high neutron yield (shown in Fig. 8), the high voltage signal exhibits a single peak indicating a single compression. The neutron yield for this discharge is 1.4×10^8 higher than the average value. The plasma column is broken at three places due to the development of the $m = 0$ instability. The time resolved hard X-ray signal is saturated and it appears immediately after the maximum compression ($t = 0$). About 100 ns after the compression, there is a neutron signal and lasts for about

Fig. 5 A three frame sequence of a discharge during the pre-focus and focus phase along with signal profiles of dY_N/dt , dY_{HX}/dt , dY_{SX}/dt and V . The neutron yield for this discharge is 4.3×10^7 lower than the average value

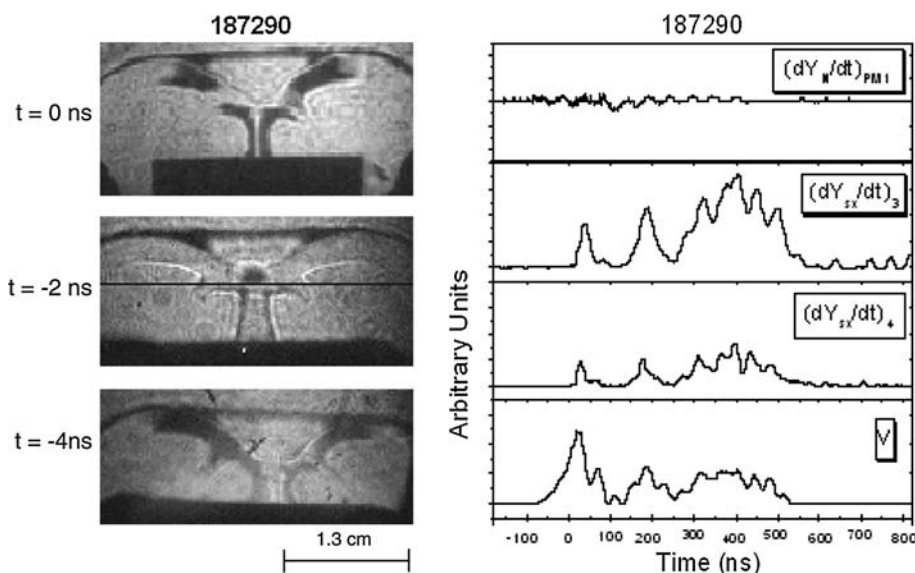


Fig. 6 A three frame sequence of a discharge low neutron yield (2.4×10^7) during the pre-focus and focus phase along with signal profiles of dY_N/dt , dY_{HX}/dt , dY_{sx}/dt and V

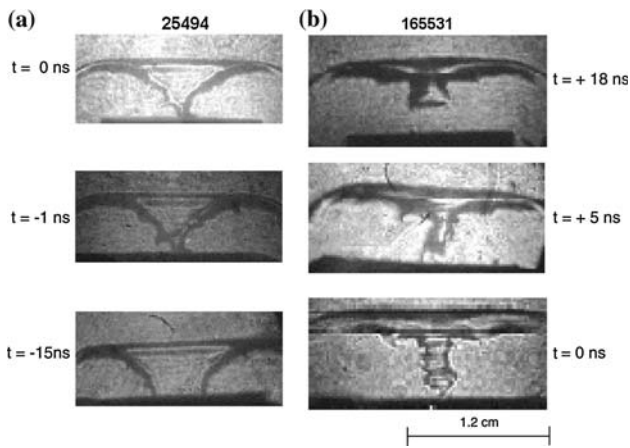
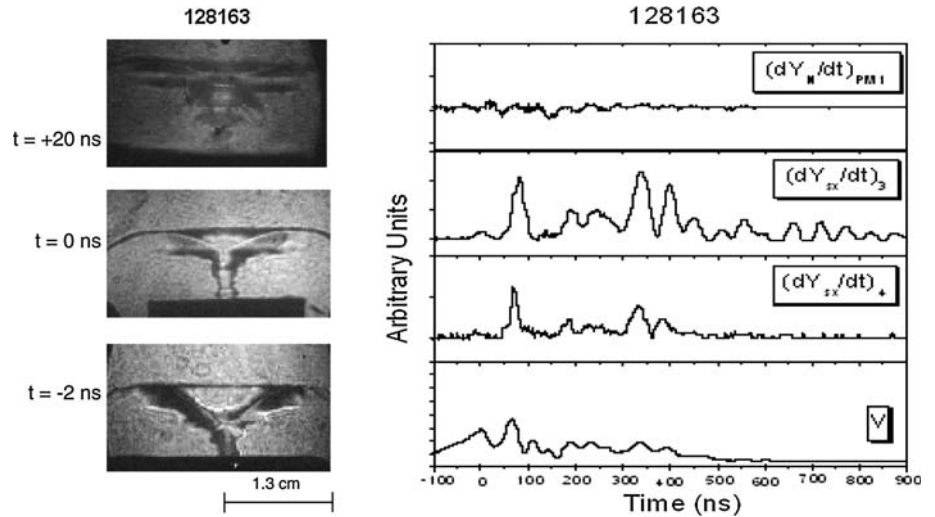
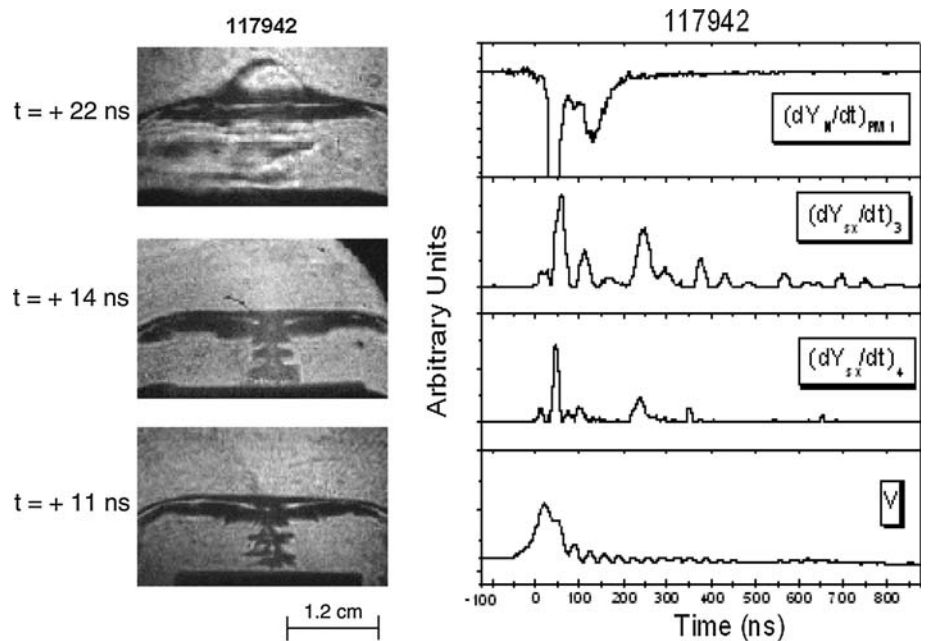


Fig. 7 Three frame sequence of two discharges with average neutron yield during the pre-focus, focus and post focus phases (-15 to $+18$ ns)

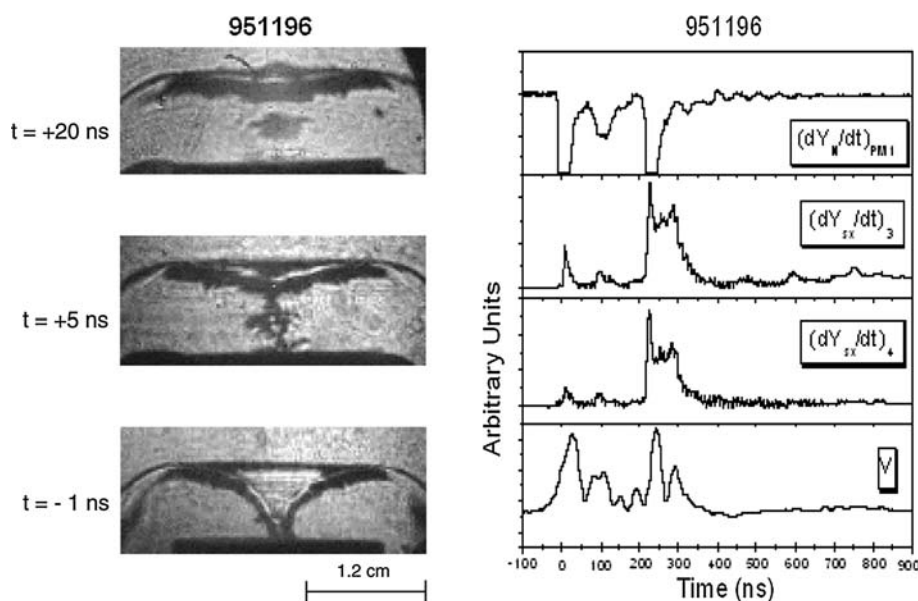
Fig. 8 A three frame sequence of a discharge during the focus phase along with signal profiles of dY_N/dt , dY_{HX}/dt , dY_{sx}/dt and V . The neutron yield for this discharge is 1.4×10^8 higher than the average value



60 ns. This signal is indicative of a set up of a strong deuteron beams under the influence of a self generated electric fields to undergo a beam target fusion.

An other three frame shadowgraph of a discharge with exceptionally high neutron yield (1.9×10^8) along with the time resolved signal profiles of hard X-rays (HX), neutrons (N), soft X-rays and high voltage is shown in Fig. 9. In the bottom frame, the left wing of the sheath seems to reach earlier than the right one. The column is broken in two places but the column seems to be compressed with an intense magnetic field. The instant at which the $m = 0$ instability starts to destroy the column, the neutron and X-rays emission begins. The breaking up of the column is characterised also by the development of micro instabilities.

Fig. 9 A three frame sequence of a discharge with exceptionally high neutron yield (1.9×10^8) during the focus phase along with signal profiles of dY_N/dt , dY_{HX}/dt , dY_{SX}/dt and V



The breaking up may also correspond to the density fluctuation connected with the micro turbulences. When the filament breaks up, the spectral analysis [21] of the scattered light indicates that the ion velocity distribution is no longer Maxwellian. Simultaneously, its intensity increases beyond the thermal level and this fact can be used to study the development of the micro instabilities in the plasma. These instabilities are attributed to the current which flows on the axis. The current creates a drift between the electrons and ions. The instabilities are related to the drift velocity as $V_D = 1/n_e e$. This means that with the increase of the drift velocity, the instability growth increases. In other words, the greater the drift velocity between the ion and electron, the greater the number of break-ups and higher the radiation output. Our data agrees with this assumption, because more than 80% of the recorded discharges with the high neutron yield show 2 and sometimes 3 break-ups.

The impedance of the plasma sheath consists of the inductance $L(t)$ and the resistance $R(t)$. Both vary during the propagation and the radial compression. The voltage between the two electrodes across the insulator is $V = d(LI)/dt + RI$. From the values given by magneto-hydrodynamics computation for the electron temperature and the filament diameter, the resistance term is negligible compared to the inductance term. It is known, however, that the instabilities can increase the resistivity well above the Spitzer's expression for the plasma in equilibrium [21]. The dissipation process caused in the thermal plasma by collisions of the current driven electrons can be enhanced when instabilities occur. The anomalous resistance is caused by the collisions of the electrons with the waves when they reach high intensity level. A typical problem in

the plasma focus studies is the role played by the anomalous resistivity in heating the plasma. This is important in heating the plasma in the connective phase of the discharge, following the break ups. This plasma appears to act as a source of deuterons, which are accelerated axially into the plasma formed further away from the anode, and produce neutrons.

Post-Focus Phase

After the compression, the plasma column decays. The decay time depends on the development of the instabilities during the pinch phase.

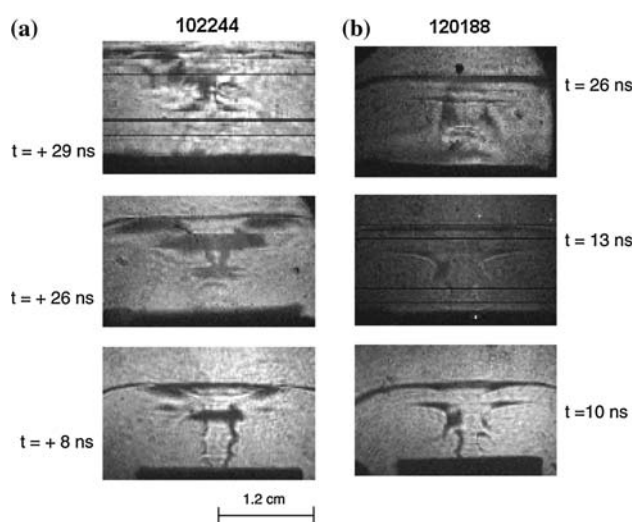


Fig. 10 Three frame sequence of two discharges during the post-focus phase. Both discharges have low neutron yield (a) 3.6×10^7 and (b) 2.8×10^7

Figure 10a, b shows shadowgraphs of two discharges with low neutron yield (3.6×10^7 and 2.8×10^7 respectively). There are distinct ripples formed along the length of the plasma column (Fig. 10a). These kind of ripples are well known and were reported by Herold et al. from schlieren pictures [22]. These ripples are caused by flute instabilities during the compression or at the later stage. The kinks are seen on both sides of the surface of the column. This kind of ripples could also be caused by the $m = 0$ instability, because in the middle and the top frame it seems that the column breaks up in the same manner as it does for the $m = 0$ instability. These ripples might have

been developed from primary current sheath ripples maintained during the maximum compression.

In Fig. 10b, the column has a broken surface on both the sides (bottom frame). It seems that this kind of ripple is a continuity of a RT instability developed during the initial stage of the radial phase. The signs of the development of the $m = 0$ instability is also seen in the same frame. At the later stage of the pinch phase (middle and top frame), the column is broken due to the $m = 0$ instability. It appears that this kind of discharges are neither suitable for the neutron yield, nor for the X-ray production. However, the percentage of this kind of discharges is very low.

Fig. 11 A three frame sequence of a discharge during the post-focus phase along with signal profiles of dY_N/dt , dY_{HX}/dt , dY_{SX}/dt and V . The neutron yield for this discharge is 1.63×10^8 higher than the average value

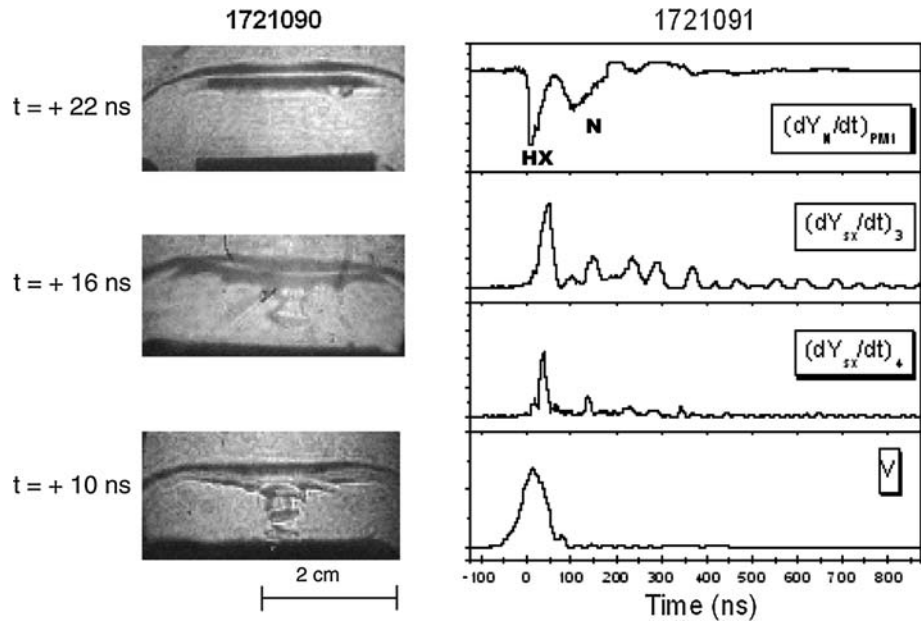


Fig. 12 A three frame sequence of a discharge 500 ns after the first compression. This discharge exhibits a second focusing event

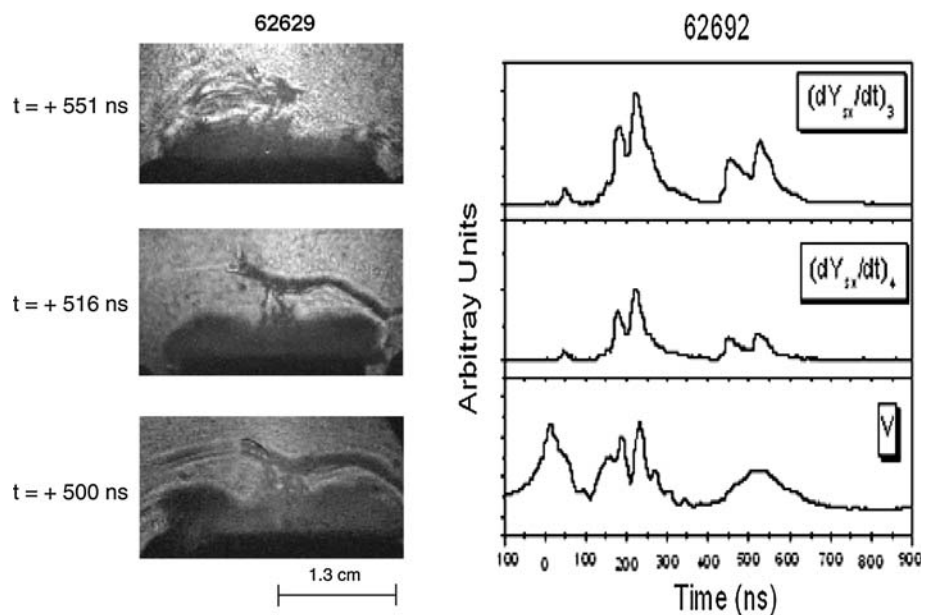


Figure 11 shows a sequence taken during the post-focus phase along with the time resolved signal profiles of hard and soft X-rays, neutrons, high voltage probe and Rogowski coil. The neutron yield for this discharge is 1.63×10^8 higher than the average value. This discharge corresponds to a single compression regime. Time resolved hard X-rays appear exactly at the time of the compression indicating the generation of energetic electrons responsible for the production of hard X-rays. The neutron signals appears 60 ns after the compression again explaining the generation of strong deuteron beams and producing these neutron via beam target mechanism. As far as the soft X-rays are concerned, a single burst is seen a few ns after the compression which is attributed to the low energy remnant electrons after producing hard X-ray burst.

The plasma column in this figure is broken only on one side (bottom frame). This might be the combination of the $m = 0$ and $m = 1$ instabilities occurring simultaneously. The magnetic field might be acting in such a manner that the column is compressed only on one side.

Figure 12 shows an interesting sequence taken 500 ns after the maximum compression. In this discharge, a second focused column, along with the emission of the copper vapours is seen. The voltage probe signal shows a hump at the instant at which the shadowgraph is taken (+500 ns). This clearly indicates the existence of the second compression at this instant. The column is diffused and the current sheath is asymmetrical. There is also a soft X-ray emission during this time. This emission is partly due to the copper vapours from the anode material.

Conclusions

The correlation of shadowgraphic images of the focus with the high voltage probe signal, together with the X-ray and neutron emission characteristics, enabled us to identify the important regimes of the focus. The focus operates in two regimes namely; the single compression regime and the multiple compression regime. The multiple compression regime is indicative of the low radiation output, especially the neutron and hard X-ray and is supportive to the soft X-rays whereas the single compression regime is best suited for the high neutron and hard X-ray output.

For the discharges with low neutron yield the sheath is not smooth and the radial compression does not favour the high dense column formation with no disturbances due to instabilities. Whereas, for the discharges with high neutron

yield, there is multiple break ups of the plasma column due to on set of $m = 0$ instability which favours the high density plasma and in turn the high neutron and hard X-ray output. However, the soft X-ray out put is relatively higher for the discharges with low neutron yield or vice versa. Therefore, the conditions for the plasma focus to operate in the neutron-optimized mode are different from that for the soft X-ray optimized mode.

During the initial stage of the radial phase the sheath moves with velocities ranging from 10–23 cm/ μ s while at later stages (up till the maximum compression), the velocities reach 32–42 cm/ μ s.

References

1. J.O. Pouzo, M.M. Milanese, IEEE Trans. Plasma Sci. **31**, 1237 (2003)
2. M. Zakaullah, K. Alimgir, M. Shafique, S.M. Hassan, M. Sharif, S. Hussain, A. Waheed, Plasma Source Sci. Tech. **11**, 377 (2002)
3. H. Bhauyan, S.R. Mohanty, N.K. Neagy, S. Bujarbarua, R.K. Rout, J. Appl. Phys. **95**, 2975 (2004)
4. M. Zakaullah, A. Alimgir, M. Shafique, M. Sharif, A. Waheed, IEEE Trans. Plasma Sci. **30**, 2089 (2002)
5. M. Shafique, S. Hussain, A. Waheed, M. Zakaullah, Plasma Source Sci. Tech. **12**, 199 (2003)
6. M.S. Rafique, A. Serban, P. Lee, S. Lee, 26th EPS Conference on Contr. Fusion and Plasma Physics, ECA 23J 1249, 1999
7. S.V. Springham, S. Lee, M.S. Rafique, Plasma Phys. Cont. Fusion **42**, 1023 (2000)
8. J.W. Mather, Phys. Fluids **8**, 366 (1965)
9. W.H. Bostick, V. Nardi, W.J. Prior, J. Plasma Phys. **8**, 7 (1972)
10. K.H. Schonabach, L. Michel, H. Fischer, Appl. Phys. Lett. **25**, 574 (1974)
11. J.P.J. Rager, in *Proceedings 3rd Topical Conference on Pulsed High β Plasmas*, C1.3, 1975
12. B. Naharath, IPF Report 78-1, 1978
13. T. Yamamoto et al., Japn. J. Appl. Phys. **23**, 242 (1984)
14. N. Toshikazu et al., Japn. J. Appl. Phys. **24**, 324 (1985)
15. G.G. Comisar, Phys. Fluids **12**(5), 1000 (1969)
16. M.A. Muhammadi, R. Verma, S. Sobhanian, C.S. Wong, S. Lee, S.V. Springham, T.L. Tan, P. Lee, R.S. Rawat, Plasma Source Sci. Tech. **16**, 785 (2007)
17. M.S. Rafique, PhD. Thesis, NIE/NTU Singapore, 2000
18. R.S. Rawat, T. Zhang, C.B.L. Phua, J.X. Then, K.A. Chandra, X. Lin, A. Patran, P. Lee, Plasma Source Sci. Tech. **13**, 569 (2004)
19. S. Lee, A. Sernan, IEEE Trans. Plasma Sci. **24**, 1101 (1996)
20. T. Zhang, R.S. Rawat, S.M. Hassan, J.J. Lin, S. Mahmood, T.L. Tan, S.V. Springham, V.A. Gribkov, P. Lee, S. Lee, IEEE Trans. Plasma Sci. **34**, 2356 (2006)
21. A.G. Tolstolutski, I.M. Zolotrubov, V.G. Zykov, M.Y. Novikov, V.S. Demin, Sov. J. Plasma Phys. **8**(2), 141 (1982)
22. H. Herold et al., in *Proceedings 9th International Conference on Plasma Physics and Contrl. Nucl. Fusion and Res.*, Baltimore, 1982, CN-41/N-6-1